**OPEN**

# Metamaterials with conformational nonlinearity

Mikhail Lapine[1,2], Ilya V. Shadrivov[1,2], David A. Powell[1] & Yuri S. Kivshar[1,2]

[1]Nonlinear Physics Center, Research School of Physics and Engineering, Australian National University, Canberra ACT 0200, Australia, [2]National Research University for Information Technology, Mechanics and Optics (ITMO), Saint Petersburg 197101, Russia.

Within a decade of fruitful development, metamaterials became a prominent area of research, bridging theoretical and applied electrodynamics, electrical engineering and material science. Being man-made structures, metamaterials offer a particularly useful playground to develop interdisciplinary concepts. Here we demonstrate a novel principle in metamaterial assembly which integrates electromagnetic, mechanical, and thermal responses within their elements. Through these mechanisms, the conformation of the meta-molecules changes, providing a dual mechanism for nonlinearity and offering nonlinear chirality. Our proposal opens a wide road towards further developments of nonlinear metamaterials and photonic structures, adding extra flexibility to their design and control.

Metamaterials — artificial materials designed to deliver an unusual electromagnetic response — have already established a prominent area of theoretical and experimental physics[1,2] with applications ranging from super-imaging[3] and transformation optics[4] to tunable and active materials[5], photonics[6] and plasmonics[7]. At the same time, the corresponding ideas were readily adopted in acoustics, promising unusual mechanical behaviour[8,9]. Clearly, simultaneous access to electromagnetic, mechanical and thermal properties offers great application capabilities, as demonstrated, e.g. by mechanically tunable[10] and thermally reconfigurable[11,12] metamaterials. Such a connection has been so far achieved by engineering the metamaterial structure so as to provide an artificial means to control electromagnetic properties; this approach is useful for tunability, however, it does not provide a dynamic interaction.

Here we design a simple metamaterial element where responses of a different nature are intrinsically coupled through its very structure. Such an element is readily found as a thin wire wound into a spiral (Fig. 1). From an electromagnetic perspective, it is a resonator with chiral properties, and from a mechanical perspective it is a spring. Finally, its specific shape makes all the characteristics sensitively depending on temperature. This natural "coincidence" is of a great use as soon as the parameters of the spiral allow thermo-magneto-mechanical coupling, which results in efficient changes of its conformation. Indeed, an external electromagnetic wave induces a current along the spiral conductor, but this current causes an attractive force between the windings. The spiral will therefore contract until that force is balanced by the spring force, however the corresponding change in spiral geometry will shift the resonance and thus alter the current amplitude in a self-consistent manner. In addition, the thermal expansion of the spiral, resulting from its heating with the increasing incident power, provides a relevant contribution, further shifting the resonance — importantly, in the same direction. This dual conformational feedback leads to exotic nonlinear behaviour.

Spirals are chiral resonant particles known for about a century[13], being suitable for producing bi-isotropic[14] or bi-anisotropic[15] media, depending on how they are arranged in space. Approximate models were developed to derive polarizability of simplified canonical spirals[16], which can be used to derive effective parameters of dilute media, as well as for bi-anisotropic lattices of infinite spirals[17]. However, in the general case, the analysis of a periodic or random lattice of volumetric spiral scatterers eludes analytical treatment. For this reason, in the qualitative analysis in this paper we assume that the individual elements are arranged in such a way as to minimize mutual interaction so that the mutual coupling would only manifest itself in a small shift of the resonance frequency[18]. We can therefore retrieve all the qualitative features by analysing the response of an individual spiral.
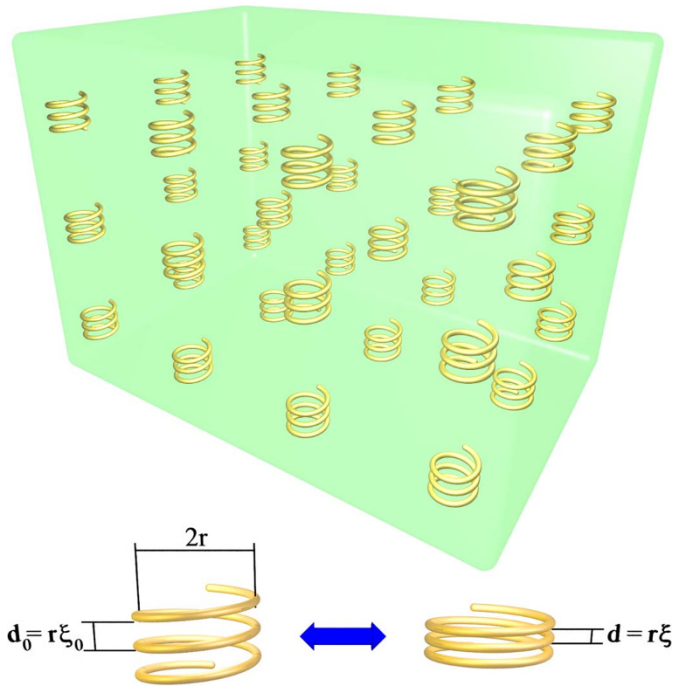
## Results

**Governing equations.** Nonlinear behaviour of the metamaterials made of spiral meta-molecules can be theoretically understood as its resonance frequency essentially depends on the spiral pitch $\xi$ as well as on the radius of the spiral $r$. Accordingly, the resonance shifts when the spiral compresses in response to attraction between the

**Figure 1 | Schematic of a metamaterial composed of spiral meta-molecules.** The structural units are electromagnetic resonators which can change their geometrical conformation: spiral pitch $\xi$ can vary, following a balance between the attractive force induced by magnetic field and the spring rigidity; and spiral radius $r$ can change upon thermal expansion.

windings as well as when a thermal expansion occurs due to heating, both the effects triggered by the induced currents. This ensures the intensity-dependent phenomena, providing for essential nonlinearity, for example, in dependence of the induced magnetization on the incident magnetic field. We note that the change in spiral pitch $\xi$ manifests itself with the corresponding change of its chiral properties. We can qualitatively describe the degree of chirality with the ratio between the electric $p_z$ and magnetic $m_z$ moments, induced in each spiral along its axis $z$. This ratio is directly determined by the geometry of the spiral[17], $|\gamma| = |p_z/m_z| = \xi/\omega\pi r$.

Precise electromagnetic modelling of a multi-turn finite spiral is known to be analytically challenging, however for a good qualitative description of the nonlinear phenomena, we can rely on a simple circuit model[19] which is applicable to two-windings spiral resonators if their resonance frequency is well within the quasi-static regime (see *Methods*).

For small $\xi$, the Ampère force acting between the windings of the spiral, can be calculated as that between the two parallel wires of the corresponding length. Given the actual current distribution along the entire spiral[19], we have found the net total force acting between the windings to be $F_u = \mu_0 I^2/12\xi$. This attractive force is be countered by the spring force $F_s$ (see *Methods*). The mechanical equilibrium is thus governed by

$$3Gr^2w^4(\xi - \xi_0)\xi + 2\mu_0 I^2 = 0, \tag{1}$$

which may seem to be a quadratic equation for $\xi$, however it is in fact far more complicated as the current $I$ also depends on $\xi$ and $r$ through the impedance equation:

$$\left(R(r) + i\omega L(r) - \frac{i}{\omega C(r, \xi)}\right) \cdot I = -i\omega\mu_0\pi r^2 H_0. \tag{2}$$

Here, $H_0$ is the amplitude of the magnetic field of the incident wave (we imply the incident polarization with $\mathbf{H}_0$ being parallel to the spiral axis).

The thermal behaviour of the spiral is provided by its expansion (so that in the above equations, $r$ depends on the temperature $T$) as

well as by the temperature dependence of its conductivity (see *Methods*). The amount of heat $Q^+ = RI^2/2$ which is realized per second in the spiral, is balanced, in a thermal equilibrium, to the heat loss through its surface. Precise dynamics of spiral cooling is complicated, and cannot be easily described by radiative emission ($\propto T^4$); for our qualitative purposes we assume, to a first approximation, that the heat loss depends on the temperature increase $\Delta T$ as $Q^- = \beta \cdot 2w(2\pi r)^2 \cdot \Delta T$, where $\beta$ is an empirical coefficient. Thus, equations (1), (2) and

$$\beta \cdot 2w(2\pi r)^2 \cdot \Delta T = RI^2/2 \tag{3}$$

form a system of coupled equations, which can be numerically solved for $\xi$, $\Delta T$ and $I$ at a given frequency $\omega$ and amplitude $H_0$ of the incident field.

**Nonlinear characteristics.** For a physical representation of the arising nonlinearity, we can evaluate the total magnetic moment, induced in each spiral, and obtain the effective magnetization of the metamaterial, $M = I v\pi r_0^2$ (where $v$ is the volumetric concentration of spirals).

In Fig. 2 a–c, we illustrate the amplitude-dependent phenomena observed when the signal frequency is slightly lower than $\omega_0$. With the increase of power, the spiral compression enhances the
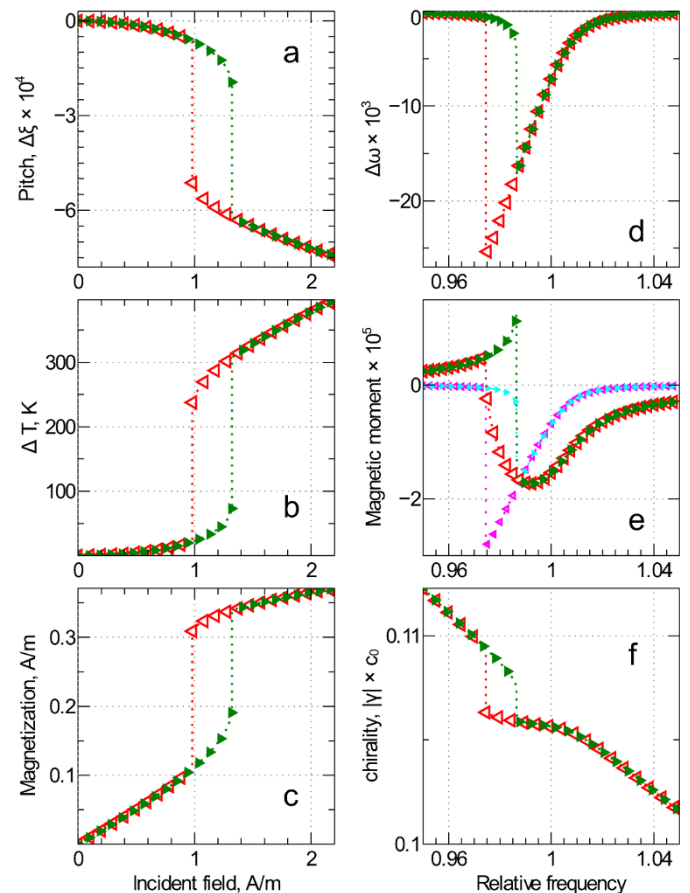


**Figure 2 | Various characteristics of the conformational nonlinearity.** Dependence of the metamaterial properties on (a–c) the incident amplitude $H_0$ (at the relative frequency of $0.99\omega_0$), or (d–f) on the signal frequency (with the amplitude 2 A/m), for relaxed (right-pointing green triangles) and compressed (left-pointing red triangles) conformations. Panel (a) shows the change in spiral pitch $\Delta\xi$; panel (b) the increase in spiral temperature $\Delta T$, panel (c) the absolute value of the effective magnetization, panel (d) the relative shift in the resonance frequency $\Delta\omega$, panel (e) the magnetic moment (real and imaginary parts) of a single spiral, and panel (f) the chirality parameter $\gamma \cdot c_0$.

resonance, and therefore a positive feedback occurs upon a certain threshold, when the spring force becomes insufficient to hold the resonantly growing attraction [follow the green right-pointing triangles in Fig. 2a]. The spiral then jumps to another conformation, where a stronger compression shifts the resonance sufficiently below the signal frequency, so that the induced force becomes weak again, and further increase in power causes slow growth in magnetization. However, if the field intensity is decreased from the high values, the spiral remains in a compressed conformation longer, as it is now trapped near the resonance. It is only released when the peak amplitude of force is insufficient to hold it [follow the red left-pointing triangles in Fig. 2a]. Further contribution is provided by the thermal expansion of the spiral heated by the currents (Fig. 2b). The two effects act simultaneously, providing a remarkable hysteresis-like pattern for all the macroscopic properties of the metamaterial, such as magnetization (Fig. 2c).

Two conformations can be also observed when the frequency of the incident radiation is varied (Fig. 2 d–f). When the signal frequency increases at a given amplitude, the spiral remains just slightly compressed until, close to the initial resonance $\omega_0$, the attractive force becomes strong enough to trigger a jump to a compressed conformation (so that the spiral resonance goes below the signal frequency), and further frequency increase relaxes this compression. With decreasing frequency, the resonance of the spiral is already below the signal, so approaching it steadily increases attractive forces and the spiral undergoes continuous compression, led by the slope of the resonance. To illustrate the frequency-dependent phenomena, we show how the resonance frequency (Fig. 2d), the magnetic moment (Fig. 2e), and the chirality (Fig. 2f) vary in hysteresis-like loops.

For the proof-of-principle experiments in the microwave range, we take a thicker wire, such that the thermal effect dominates. Fig. 3(a) shows the transmission amplitude as a function of input frequency and power. It can be seen that there is a substantial shift of the resonance to lower frequencies as the input power is increased. As can be seen in Fig. 3(b), the maximum frequency shift is less than the width of the resonances, which is insufficiently strong to observe bistability. Figure 3(c) shows a shift of the resonant frequency as a function of the input power. Analysis of this shift allows to estimate the coefficient in Eq. (3) which determines the effective heat loss from the spiral, which turns out to be about $\beta \approx 40 \pm 10$. We have used this coefficient for the above theoretical calculations.

## Discussion

The above results demonstrate that the flexible spiral resonator exhibits nonlinear behaviour through the conformational changes of its meta-molecules. In particular, the resulting metamaterial features a nonlinear chiral response. The conformational dynamics of the spiral is most interesting when the thermal and mechanical reactions are comparable to each other, as shown with our theoretical examples.

Among the parameters of the spiral, the relative wire thickness $w$ has the most drastic effect on the interplay between the mechanical response (which increases as the fourth power of $1/w$) and the thermal effect (largely independent of $w$). Clearly, to ensure sufficiently strong force between the current loops, the windings of the spiral have to be close to each other, $\xi \ll 1$, while the wire should be thin enough to make the spring soft to respond to the relatively weak Ampère forces. We conclude that for the spiral's compression to dominate over its thermal expansion the relative wire width should be smaller than 0.01.

Our proposal provides a starting platform for further analysis of the nonlinear phenomena in various metamaterials based on the flexible chiral particle, which can be made bi-isotropic, bi-anisotropic and even non-chiral, by choosing an appropriate lattice and alignment. While a lot of peculiar features will be provided with the arising mutual interactions, the essence of nonlinear response is determined by the properties of an individual spiral particle, and therefore the above analysis forms a basis for further research as well as for development of useful applications.
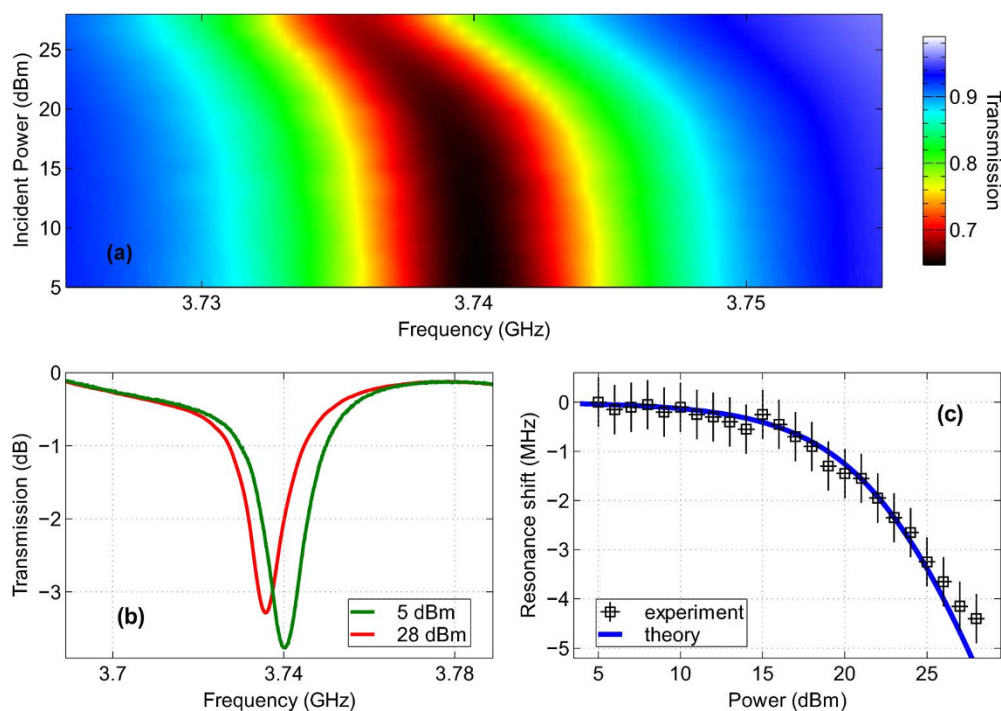


**Figure 3 | Experimental results.** Panel (a) shows transmission through the spiral in the waveguide as a function of frequency and input power, panel (b) the curves for the highest and lowest measured power, panel (c) the frequency shift as a function of input power, with a comparison between the measurements and theoretical estimates.
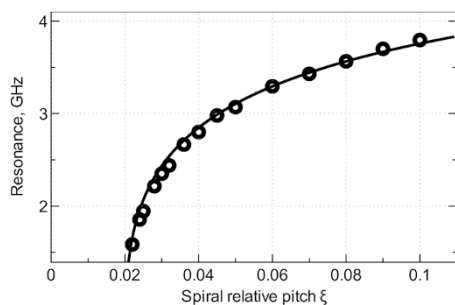
**Figure 4 | Resonance frequency of spiral resonators with different pitch $\xi$.** Comparison between the effective circuit theory (solid line) and numerical simulations (circles). Spiral parameters here are $r_0 = 2$ mm and $w = 0.01$.

## Methods

In our theoretical analysis, we use dimensionless quantities $w = r_w/r$ and $\xi = d/r$ for the radius of the wire $r_w$ and vertical distance $d$ between windings (Fig. 1), normalized to the radius $r$ of the spiral loops.

With the quasi-static model[19] the spiral is described as an *LC*-circuit, with the inductance $L$ being the same as the inductance of a single circular loop of the same wire, $L = \mu_0 r(\ln(8/w) - 2)$ (because the net current, flowing within the entire spiral — the sum over the current distribution in all turns — is uniform along the entire circumference). The latter equally applies to the resistance $R = \sqrt{\mu_0 \omega/2\sigma}/w$; both the $L$ and $R$ are taken with skin-effect in mind. The capacitance $C$ is defined by that between the two windings (with a minor correction for their curvature being negligible for small $\xi$): $C(\xi) = 2\pi\varepsilon_0 \cdot \pi r/\mathrm{acosh}(\xi/2w)$. We have checked, with the aid of numerical simulations (Fig. 4), that this simple circuit model correctly predicts the resonant frequency $\omega_r(\xi) = 1/\sqrt{L(r)C(r, \xi)}$ of two-turn spirals.

The mechanical properties of a two-windings spiral are described by the stiffness coefficient $k = Grw^4/8$, where $G$ is the shear modulus of the spiral material. Note that the characteristic frequency of mechanical oscillations, $\omega_M = w\sqrt{3G/2\rho}/(4\pi r)$ is many orders of magnitude smaller than the electromagnetic frequencies involved, so the analysis of the spiral geometrical reconfiguration is essentially static and is determined by time-averaged amplitudes of the current. The spring response is then described with the Hooke's law, so it linearly increases with the deviation from the initial pitch value $\xi_0$: $F_s = kr(\xi - \xi_0)$.

Temperature dependence of the spiral parameters is determined by a thermal expansion coefficient $\alpha$ as $r = r_0(1 + \alpha \cdot \Delta T)$. Note that it leaves $\xi$ and $w$ unchanged provided that the spiral is perfectly annealed and is free from internal stress. The electric conductivity is affected in a similar way, $\sigma = \sigma_0(1 + \eta \cdot \Delta T)$ with a temperature coefficient of conductivity $\eta$.

For theoretical calculations, we assumed $r_0 = 5$ mm, $\xi_0 = 0.04$, $w = 0.01$, and the material parameters of copper for $\sigma = 6.6 \cdot 10^7$ S, $G = 40$ GPa, $\alpha = 1.7 \cdot 10^{-5}$ K$^{-1}$ and $\eta = 4.3 \cdot 10^{-3}$ K$^{-1}$.

Numerical simulations were performed using the finite-element based frequency-domain solver of *CST Microwave Studio*. The spiral was excited by a plane wave with magnetic field parallel to the axis of the the spiral. The material was modelled as a perfect electrical conductor, and a curved mesh was used to ensure good resolution of the geometry without excessively fine meshing. The spiral was excited over a broad frequency range, and the resonant frequency was determined as that with the maximum magnitude of the normal magnetic field at the centre of the spiral.

For our experiments, the spirals were made of 100 μm-thick copper wire with 2.4 mm radius and 0.5 mm pitch. We suspend a spiral parallel to the axis of a WR 229 rectangular waveguide on a dielectric rod so that the incident magnetic field is along the spiral axis. The waveguide is excited by a vector network analyzer (Rhode and Schwartz ZVB-20) after amplification by a 1 W amplifier (HP 83020A). The output of the waveguide is measured by the network analyzer, through a 20 dB attenuator to eliminate gain compression in the detectors. To ensure that the nonlinear response of the amplifier does not contribute to the measurements, a power calibration is performed for each individual power level, thus ensuring that the power level at the waveguide input is compensated for the frequency and power dependent gain of the amplifier. A directional coupler is used to sample the output from the amplifier, so that the power calibration can be performed *in situ*, and to provide a reference level

against which to compare the output signal from the waveguide. The input power to the waveguide was varied between 5 dBm and 28 dBm in steps of 1 dB.

1. Solymar, L. & Shamonina, E. *Waves in Metamaterials* Oxford University Press, 2009.
2. Marqués, R., Martín, F. & Sorolla, M. *Metamaterials with negative parameters* Wiley, 2008.
3. Pendry, J. B. Negative refraction makes a perfect lens. *Phys. Rev. Lett.* **85**, 3966–3969 (2000).
4. Pendry, J. B., Schurig, D. & Smith, D. Controlling electromagnetic fields. *Science* **312**, 1780–1782 (2006).
5. Boardman, A. *et al.* Active and tunable metamaterials. *Lasers Photonics Rev.* **5**, 287–307 (2011).
6. Shalaev, V. M. Optical negative-index metamaterials. *Nature Photonics*, **1**, 41–48 (2007).
7. Schuller, J. A., Barnard, E. S., Cai, W., Jun, Y. C., White, J. S. & Brongersma, M. L. Plasmonics for extreme light concentration and manipulation. *Nature Materials*, **9**, 193–204 (2010).
8. Li, J. & Chan, C. T. Double-negative acoustic metamaterial. *Phys. Rev. E* **70**, 055602 (2004).
9. Norris, A. N. Acoustic cloaking theory. *Proc. Royal Soc. A* **464**, 2411–2434 (2008).
10. Lapine, M. *et al.* Structural tunability in metamaterials. *Appl. Phys. Lett.* **95**, 084105 (2009).
11. Tao, H. *et al.* Reconfigurable terahertz metamaterials. *Phys. Rev. Lett.* **103**, 147401 (2009).
12. Chen, H.-T. *et al.* Tuning the Resonance in High-Temperature Superconducting Terahertz Metamaterials. *Phys. Rev. Lett.* **105**, 247402 (2010).
13. Lindman, K. F. Om en genom ett isotropt system av spiralformiga resonatorer alstrad rotationspolarisation av de elektro-magnetiska vågorna. *Öfversigt af Finska Vetenskaps-Societetens förhandlingar, A* **LVII**, 1–32 (1914).
14. Lindell, I. V., Sihvola, A. H., Tretyakov, S. A. & Viitanen, A. J. *Electromagnetic waves in chiral and bi-isotropic media* Artech House, Boston and London, 1994.
15. Serdyukov, A., Semchenko, I., Tretyakov, S. & Sihvola, A. *Electromagnetics of bi-anisotropic materials: Theory and applications* Gordon and Breach, Amsterdam, 2001.
16. Tretyakov, S., Mariotte, F., Simovski, C., Kharina, T. & Heliot, J.-P. Analytical antenna model for chiral scatterers: comparison with numerical and experimental data. *IEEE Trans. Antenn. Propag.* **44**, 1006–1014 (1996).
17. Belov, P. A., Simovski, C. R. & Tretyakov, S. A. Example of bianisotropic electromagnetic crystals: The spiral medium. *Phys. Rev. E* **67**, 056622 (2003).
18. Gorkunov, M., Lapine, M., Shamonina, E. & Ringhofer, K. H. Effective magnetic properties of a composite material with circular conductive elements. *Eur. Phys. J. B* **28**, 263–269 (2002).
19. Baena, J. D., Marqués, R., Medina, F. & Martel, J. Artificial magnetic metamaterial design by using spiral resonators. *Phys. Rev. B* **69**, 014402 (2004).

## Author contributions

The design was developed by M.L. and I.V.S and discussed by all the authors. Theoretical analysis was made by M.L., experiments were carried out by I.V.S., and numerical simulations were performed by D.A.P. All the authors have analysed and discussed the results. The manuscript was written by M.L., Y.S.K., D.A.P. and I.V.S. and the figures prepared by I.V.S., D.A.P. and M.L.

## Additional information